JACS
JOURNAL OF THE AMERICAN CHEMICAL SOCIETY
Communication
pubs.acs.org/JACS

Packing Interactions in Hydrated and Anhydrous Forms of the Antibiotic Ciprofloxacin: a Solid-State NMR, X-ray Diffraction, and Computer Simulation Study

Luís Mafra,*[,†,‡] Sérgio M. Santos,[†] Renée Siegel,[†] Inês Alves,[†] Filipe A. Almeida Paz,[†] Dmytro Dudenko,[‡] and Hans W. Spiess[‡]

[†]Department of Chemistry, CICECO, University of Aveiro, 3810-193 Aveiro, Portugal, and
[‡]Max-Planck-Institut für Polymerforschung, Ackermannweg 10, 55128 Mainz, Germany

Supporting Information

ABSTRACT: We present an experimental NMR, X-ray diffraction (XRD), and computational study of the supramolecular assemblies of two crystalline forms of Ciprofloxacin: one anhydrate and one hydrate forming water wormholes. The resonance assignment of up to 51 and 54 distinct ^{13}C and ^{1}H resonances for the hydrate is reported. The effect of crystal packing, identified by XRD, on the ^{1}H and ^{13}C chemical shifts including weak interionic H-bonds, is quantified; ^{1}H chemical shift changes up to ∼−3.5 ppm for CH···π contacts and ∼+2 ppm ($CH\cdots O^{(-)}$); ∼+4.7 ppm ($^{(+)}NH\cdots O^{(-)}$) for H-bonds. Water intake induces chemical shift changes up to 2 and 5 ppm for ^{1}H and ^{13}C nuclei, respectively. Such chemical shifts are found to be sensitive detectors of hydration/dehydration in highly insoluble hydrates.

Understanding how molecular systems self-assemble in the solid-state continues to be a challenge. In this regard, H-bonding and van der Waals interactions are considered to play major roles as structure-driving entities in the construction of supramolecular arrangements.[1,2] This is of particular relevance in pharmaceutical sciences, as multiple crystal forms of the same active pharmaceutical ingredient (API) occur frequently, posing diverse problems in the pharmacokinetics, stability, and formulation of drugs. Here, we investigate in detail packing interactions of different types such as weak/strong H-bonds and $\pi\cdots\pi$ interactions in one anhydrate and one hydrate form of Ciprofloxacin (CIP) (Figure 2f), a fluoroquinolone API, combining XRD with high-resolution solid-state NMR spectroscopy and computer simulations, emphasizing the effect of nonconventional H-bonds[1] and water on NMR chemical shifts.

Weak CH···X contacts represent an intriguing aspect of supramolecular assemblies.[1] In solids, only a few examples exploiting NMR chemical shifts have been reported for studying CH···O and CH···N H-bonds. In general, quantification of weak intermolecular interactions represents a challenge for computational and experimental characterization.[3−5] In contrast to strong/moderate H-bonds with energies of −5 to −40 kcal·mol^{-1}, CH···π contacts have a negligible impact (−1 to −5 kcal·mol^{-1}), and little is known about their structural role in solids. They are often neglected when discussing molecular assemblies.[6] Recently, however, CH···π contacts have been identified in protein-pharmaceutical complexes.[7] In our case, the structures of both anhydrous and hydrated forms of CIP can be determined by single-crystal XRD. NMR chemical shifts, however, depend on the electronic environment of the nucleus studied. This gives us the unique opportunity to quantify the effect of the packing on the chemical shifts in such a complex system, to be used in related cases, where the structure is not known. Moreover, by *in silico* computer simulation, we can quantify the energetics of the different contributions to the packing.

CIP is a widely prescribed synthetic chemotherapeutic antibiotic approved for the treatment of several types of bacterial infections.[8] Despite this, its structural variety has not been investigated in sufficient detail. CIP is also one of the most water-insoluble fluoroquinolone APIs available (∼0.08 mg·L^{-1}). In contrast, other structurally similar fluoroquinolones (e.g., Norfloxacin) show solubility in water higher than 300 mg·L^{-1} [8] and exhibit up to six distinct hydrates. Despite the difficulty in producing well-defined CIP hydrates (only one, the hexahydrate, is reported: COVPIN[9]) we were able to isolate and determine the structure of two new CIP channel hydrates (forms **II** (Figures S1 and S6) and **III** (Figures S2 and S7), both triclinic $P\bar{1}$, Table S1) and to investigate their packing interactions. As **II** (3.7 hydrate) and **III** (4.8 hydrate) hold the same framework but differ in their water stoichiometries, only hydrate **II** is discussed in detail here. Water often converts anhydrates into undesirable hydrates during storage or drug formulation. In fact, water penetrates the CIP lattice (forms **II**) by simple exposure of **I** to water vapor (RH > 90%) [method 2]. This intriguing observation prompted us to specify the molecular interactions that intervene in the structural reorganization upon water intake/removal in its anhydrous/hydrated packing, via NMR chemical shifts. Form **I** also transforms into **II** upon suspension of **I** in water (method 1). Both preparation methods are described in the Supporting Information (SI). Variable temperature powder X-ray data (Figure S13) show that **II** transforms back to **I** at ∼60 °C.

Each CIP molecule in **I** (Z' = 1, UHITOV[10]) is part of a dimer with close CH···π contacts of 2.44 Å (Figure 1b) as well as in the formation of a second slipped-antiparallel dimer, glued through $\pi\cdots\pi$ interactions (Figure 1c) involving the fluorinated

Received: September 19, 2011
Published: November 28, 2011

   dx.doi.org/10.1021/ja208647n | J. Am. Chem.Soc. 2012, 134, 71−74

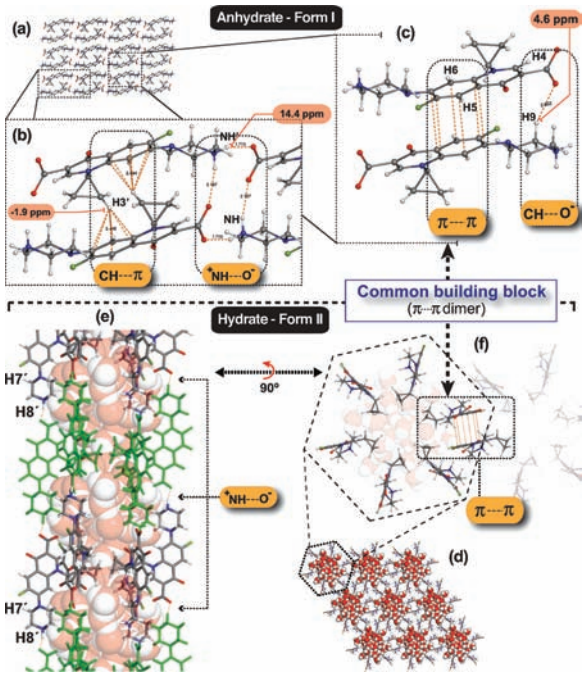

Figure 1. Crystal packing overview of **I** (top) and **II** (bottom) CIP forms showing (a, d) the full crystallographic arrangement along one of its axes directions and (c–f) the detailed views outlining specific packing interactions. (b) CIP tetramer involving two CH···π dimers; (c, f) a CIP π···π dimer; (e) water channel surrounded by six 1D CIP molecular chains connected through $^{(+)}$N···H$^{(-)}$ H-bonds. For the sake of clarity CIP residues are shown in alternated colors in (e).

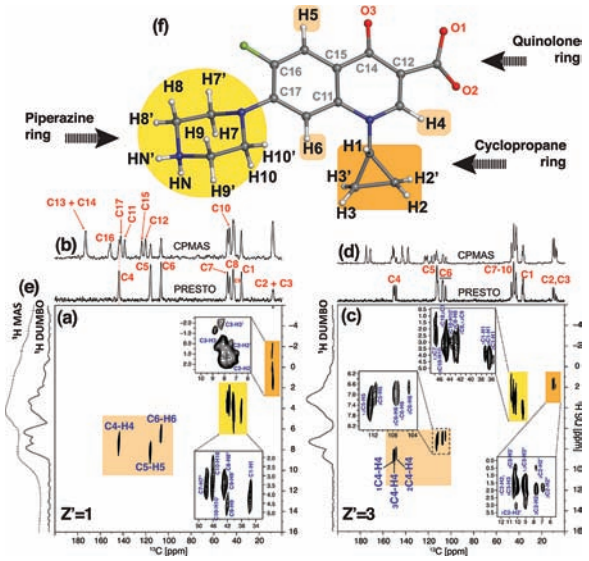

Figure 2. 2D ^{1}H–^{13}C PRESTO-HETCOR of CIP forms (a) **I** and (c) **II** recorded at 800 MHz. (b, d) ^{13}C CPMAS spectra recorded at 400 MHz. (e) ^{1}H MAS and wDUMBO[13] spectra of **I** are shown for comparison with the F1 projection of (a). Additional details are described in the SI. (f) Labeling scheme adopted for CIP. The capability of PRESTO transfer[14] to select only the directly bonded C–H is manifested by comparison with the ^{13}C CPMAS spectra [i.e., (a, c) vs (b, d); for further discussion, see the SI).

aromatic rings (separated by *ca.* 3.32 Å). The infinite stacks built from these two interleaved dimers form a 3D structure through a network of strong and weak H-bonds (Figure 3).

Form **II** self-assembles into an elaborated hexagonal arrangement of six CIP molecules (Z' = 3) accommodating a 1D water channel (Figure 1e) with highly organized interchained $(H_2O)_{22}$ water clusters formed by $(H_2O)_{14}$ inner clusters (Figure S4). Each channel is assembled by multiple H-bonds (Figure S3). Adjacent hexagons form three crystallographically distinct CIP π···π dimers that we dub as 1···1, 2···2, and 3···3. **II** belongs to a rare class of hydrates hosting confined water in channels[11,12] forming wormholes. Channel hydrates can also accommodate water molecules in continuously changing stoichiometries.

The NMR analysis of the complex packings in forms **I** and **II** requires detailed spectral assignments for ^{1}H and ^{13}C, as described in great detail in the SI. The complete ^{13}C resonance assignment of **I** (17 carbons) is depicted in the ^{13}C CPMAS and ^{1}H–^{13}C PRESTO-HETCOR NMR spectra (Figure 2a,b and Figure S8b); resonances are labeled following Figure 2f. The assignment of the 18 ^{1}H resonances is achieved by combining information from the 1D ^{1}H wDUMBO[13] spectrum of **I** (Figures S10 and S19), the 2D ^{1}H–^{1}H DQ CRAMPS spectra (Figures S9c and S11), and ^{1}H–^{13}C PRESTO-HETCOR MAS NMR spectra aided by GIPAW ^{1}H/^{13}C chemical shift calculations (Figure S9 and Table S4). For clarity, only selected resonance assignments are depicted in Figure 2. Computed ^{1}H chemical shifts of protons attached to mobile fragments (piperazine) and engaged in H-bonds usually fail to reproduce the experimental ^{1}H chemical shift if dynamics is not taken into account. Recalculating HN and HN′ ^{1}H chemical shifts by molecular dynamics, however, allowed a remarkably good correction of the GIPAW values (see the further discussion in the SI).

The ^{13}C CPMAS spectrum (Figure 2d and Figure S8) of **II** is substantially more challenging, as the number of resonances is tripled relative to **I**. The 2D ^{1}H–^{13}C HETCOR spectrum is able to discriminate all of the CH and CH_2 carbons and protons for the three distinct CIP residues, except for the overlapped region between 42 and 48 ppm from the piperazine portion. For example, the three aromatic CH protons ($_{1,2,3}$H4, $_{1,2,3}$H5, and $_{1,2,3}$H6) and the five CH/CH_2 cyclopropane protons ($_{1,2,3}$H1, $_{1,2,3}$H2, $_{1,2,3}$H2′, $_{1,2,3}$H3 and $_{1,2,3}$H3′) of each CIP residue in the three cystallographically distinct molecules can be directly identified from the spectrum (Figure 2c). The three distinct $^{(+)}$N–(HN′)···O$^{(-)}$ H-bonds are unambiguously assigned by combining the 1D ^{1}H wDUMBO and 2D ^{1}H–^{1}H DQ CRAMPS spectra (Figures S10 and S12). Overall, 51 ^{13}C and 54 ^{1}H resonances were successfully assigned using the same methodology as for **I**. Measured and experimental ^{1}H/^{13}C chemical shifts are depicted in Tables S4–S6 and Figure S14.

As the self-assembly of the drug molecules influences the chemical environment of the atoms involved in intermolecular interactions, most of our efforts was focused on quantitatively estimating (*i*) the *packing* (CH···π, CH···O$^{(-)}$, π···π, and $^{(+)}$NH···O$^{(-)}$) interactions and (*ii*) the *hydration effects* on the ^{1}H and ^{13}C chemical shifts in **I** and **II** by means of a stepwise *in silico* crystal packing dismantlement of the solved X-ray structures as sketched in Figure S15. For the evaluation of the latter effect, chemical shifts were recalculated for **II**, with all water molecules removed *in silico* without further geometry reoptimization; for the quantification of the former effect, a 1D chain of CIP zwitterions connected through $^{(+)}$NH···O$^{(-)}$ H-bonds was stripped out from the full crystal packing (a single 1D chain for **I** and three (Z' = 3) for **II**) and chemical shifts were recalculated without further geometry reoptimization (see the SI for further details). The independent contributions

dx.doi.org/10.1021/ja208647n | *J. Am. Chem.Soc.* 2012, 134, 71–74

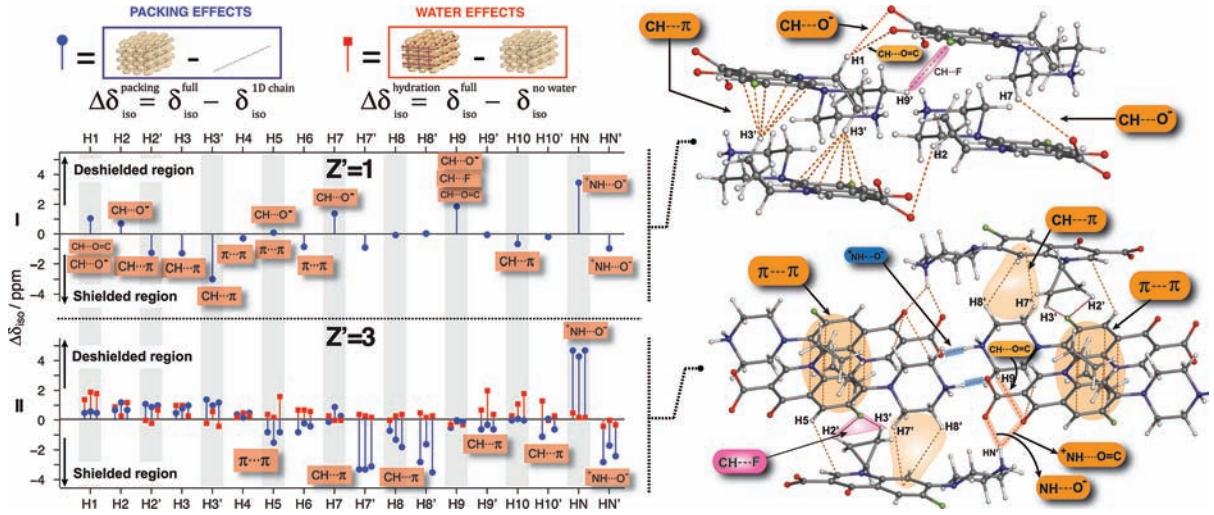

Figure 3. (Left) Stem plots showing the contribution of the crystal packing (blue stems) and water molecules (red stems) to the calculated ^{1}H chemical shifts (positive $\Delta\delta$ values indicate low-field shifts) of the ciprofloxacin forms **I** and **II**. In **II**, each of the three stems per nuclei corresponds to the crystallographically distinct CIP molecules 1, 2, and 3 (from left to right); (right) detailed view of intermolecular interactions in packings of **I** and **II**.

($\delta_{iso}^{no\ water}$ and $\delta_{iso}^{1D\text{-}chain}$) were then subtracted from the full crystal packings (δ_{iso}^{full}). The resulting chemical shift differences, $\Delta\delta_{iso}^{hydration}$ and $\Delta\delta_{iso}^{packing}$, are plotted in Figure 3 and Figure S16 as red and blue stems, respectively, for **I** and **II**, based on Tables S7 and S8. To discriminate between polarization effects (H-bonds) and intermolecular ring π-currents, $\Delta\delta_{iso}^{packing}$ values were corrected by NICS calculations[15] (Figures S17 and S18). Tables S9 and S10 compare side-by-side the values obtained by GIPAW and NICS for selected protons. Corrected $\Delta\delta_{iso}^{packing}$ values for selected packing interactions are shown in Table S11.

To mention a few examples in **I** (Figure 3), H1 and H2 show positive values around +1 ppm due to their participation in CH···O$^{(-)}$ H-bonds ($d_{H\cdots O} \approx 2.65$ Å). As they are sandwiched between two quinolone rings through CH···π contacts, a contribution of ∼−1 ppm (NICS) is included for both H1 and H2, influencing by ∼+2 ppm the *corrected* $\Delta\delta_{iso}^{packing}$ values (Table S9). In a similar way, H5 is also influenced by the π-currents and simultaneously establishes a $CH_5\cdots O{=}C-$ ($d_{H\cdots O}$ = 2.58 Å) H-bond which is shorter than the one involving H1 and H2. Yet, the $\Delta\delta_{iso}^{packing}$ value for H5 is not as deshielded as H1 and H2, because the former establishes an H-bond with a C═O acceptor (Table 1), which has a lower polarizing capacity when compared to the charged oxygen acceptors C−O$^{(-)}$. A previous study shows that H···O═C H-bonds have a deshielding effect of *ca.* +1.9 ppm for a considerably shorter distance ($d_{H\cdots O}$ = 2.16 Å).[5] The longer H···O distance observed for H5 (2.58 Å) leads to the much weaker effect in $\Delta\delta_{iso}^{packing}$ values (≈ +0.6 ppm after correction estimated by NICS, Table 1).

The ^{1}H $\Delta\delta_{iso}^{packing}$ values in the cyclopropane and aromatic regions (H1−H6) of **II** are rather low (<1 ppm) showing that these fragments are only marginally affected by the crystal packing. In contrast to **I**, these protons are not involved in CH···π or CH···O$^{(-)}$ interactions in **II**. The equatorial protons of one of the piperazine sides, H7′ and H8′ pointing out from the hexagonal 1D tube (Figure 1e), are noticeably more shielded as they are located roughly perpendicular to quinolone rings of an adjacent tube experiencing CH···π contacts in a T-shape structure (Figure 3), thus contributing with $\Delta\delta_{iso}^{packing}$ up to −4 ppm. In contrast, the two equatorial protons H9′ and H10′ at the opposite side of the ring are isolated and show $\Delta\delta_{iso}^{packing}$ values close to 0.

Table 1. NMR Quantification of Selected Crystal Packing Interactions

H-bond type[a]		Labels	Shortest Dist. / Å [H···X]	Estim. packing effect[b] (^{1}H)/ ppm
CH···π	I	H3···π	2.44	-3.1
	II	H8′···π	2.82 *(mol. 1)* 3.60 *(mol. 2)* 2.64 *(mol. 3)*	-3.0 to -3.2 -1.8 to -2.2 -3.5 to -4.0
$\pi\cdots\pi$	I	H1, H7, H9	4.11 - 4.72	-1.0 to -0.5
	II	H5	3.75 - 4.60 *(mol. 1–3)*	-1.8 to -1.0
CH···O$^{(-)}$	I	H9···(O2, O3=C)[c] H1···(O2, O3=C)[c] H5···O3=C	2.50 2.63 2.58	2.3 2.1 0.6
$^{(+)}$NH···O$^{(-)}$	I	HN···O1	2.19	3.5
	II	HN···O1	1.84 *(mol. 1)* 2.15 *(mol. 2)* 1.99 *(mol. 3)*	4.6 4.2 4.6

[a]All H-bond angles D−H···A are145°−170°. [b]Ring-current corrections (obtained from NICS) are included when applicable. [c]Bifurcated H-bonds involving two oxygen acceptors.

It is particularly interesting to investigate whether the chemically equivalent H-bonded protons, in the three distinct residues, could sense significant changes in $\Delta\delta_{iso}^{packing}$ values. This is indeed the case for the H8′ protons (Table 1 and Figure 3) due to subtle variations in the molecular conformations between residues. For instance $_{2}$H8′ is less shielded ($\Delta\delta_{iso}^{packing}$ ≈ −2.2 ppm) than $_{1}$H8′ and $_{3}$H8′ ($\Delta\delta_{iso}^{packing}$ < −3.0 ppm) because the piperazine fragment at the 2···2 dimer places $_{2}$H8′ farther away from the π-current effect of the adjacent quinolone ring ($d_{2H8'\cdots Ph}$ ≈ 5.5 Å) in comparison with the other two dimers ($d_{1,3H8'\cdots Ph}$ ≈ 4.2−4.6 Å). The adjacent $_{1,2,3}$H7′ protons are, however, affected homogeneously by the surrounding ring π-currents showing identical $\Delta\delta_{iso}^{packing}$ (Figure 1) and NICS (Figure S27) values of ∼−3.2 ppm. The packing effect on the chemical shifts of the equatorial HN′ involved in $^{(+)}$N−HN′···O$^{(-)}$ H-bonds (in both forms) yields $\Delta\delta_{iso}^{packing}$ < 0 as this interaction is never broken in our computational exercise (see SI). The geminal amine proton (HN), in axial orientation, also participates in intermolecular $^{(+)}$N−HN···O$^{(-)}$ H-bonds; the formation of this interaction translates in weakening the H-

dx.doi.org/10.1021/ja208647n | J. Am. Chem.Soc. 2012, 134, 71−74

bond involving the neighbor HN′ protons which thus appears as a negative $\Delta\delta_{iso}^{packing}$. Table 1 compiles the packing effects for selected interactions. More detail will be given elsewhere.

Our results show that the presence of water molecules in the crystal lattice of **II** changes ^{1}H and ^{13}C $\Delta\delta_{iso}^{hydration}$ shifts up to 2 and 5 ppm, respectively (Figure 3 and Figure S16). The relative changes in ^{1}H shifts are ∼4 times more important than for ^{13}C, considering the typical chemical shift spread of both nuclei (20 and 200 ppm, respectively). The majority of the observed $\Delta\delta_{iso}^{hydration}$ are positive or close to 0 (red stems in Figure 3). A good example of such a hydration effect is found for H1(cyclopropane) and H9′/H10/H10′ protons. As water is fully surrounded by these protons, they are considerably deshielded due to the polarization effect of water oxygens. The latter protons are located within the CIP tube opposite to H7′ and H8′ protons, thus interfacing the water channel as illustrated in Figure 1e. One of the CH_2 protons (axial H9) is the only one not intervening in H-bonds with H_2O, thus showing $\Delta\delta_{iso}^{hydration} \approx 0$. This illustrates that chemical shifts are a rather accurate probe of water proximity.

In pharmaceuticals, the inclusion of foreign species is, as a rule, associated with reorganization of the host framework. Here, however, **I** and **II** maintain the same $\pi\cdots\pi$ dimers (Figure 1). In an attempt to understand the reason why water molecules dispose in 1D tunnels surrounded by an hydrophobic environment without breaking up the CIP $\pi\cdots\pi$ dimers, the dimerization energies, ΔE, of the three distinct dimers of **II** were calculated and compared to the ΔE of the dimers found in **I**. The ΔE values are depicted in Figure 4. Both forms contain

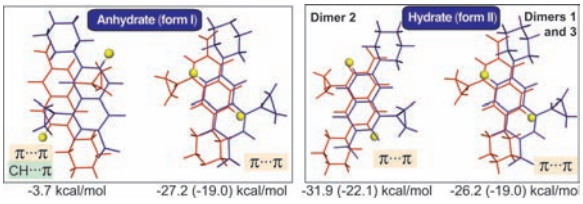

Figure 4. Computed energies of dimers formed from zwitterionic CIP species in forms **I** and **II**. Dimers 1 and 3 have almost identical $\pi\cdots\pi$ overlap. Therefore, only an average energy is given. Energies inside parentheses refer to isolated neutral dimers. Fluorine atoms are highlighted as yellow spheres.

dimers which exhibit unusually high attraction for $\pi\cdots\pi$ systems (−22.1 to −19 kcal·mol) as compared to typical $\pi\cdots\pi$ interactions (*ca.* 2−5 kcal·mol).[6] Figure 4 shows that the $\pi\cdots\pi$ dimers have similar geometrical orientations and are highly stabilized mostly by $\pi\cdots\pi$ interactions. The electric dipole−dipole interaction contributes only ∼30% of ΔE for both forms, suggesting that water intake induces the rearrangement of the lattice of **I** by preferentially disrupting the CH$\cdots\pi$ contacts, involving the sp^3 hybridized C−H3′ group, while the highly stable $\pi\cdots\pi$ CIP dimer and the $^{(+)}$NH$\cdots$O$^{(-)}$ H-bonds (connecting the CIP 1D chains) are maintained intact in **I** and **II**. Upon hydration, new CH7′$\cdots\pi$ and CH8′$\cdots\pi$ contacts are formed, exhibiting exceptional upfield shifts of −3.5 to −4.0 ppm (Table 1). Overall, the entropy of mixing is probably the main driving force for the conversion.

In conclusion, two forms [hydrate (**II**) and anhydrate (**I**)] of CIP were studied. Their structures were determined by single-crystal XRD and used as a starting point for our computational studies. The complete resonance assignment of the CIP forms was achieved combining high-resolution solid-state NMR and computational approaches. The effect of their distinct crystal packing interactions ($^{(+)}$NH$\cdots$O$^{(-)}$, CH$\cdots$O$^{(-)}$, $\pi\cdots\pi$, and CH$\cdots\pi$) on ^{1}H chemical shifts was quantified through *in silico* structure dismantlement of **I** and **II** (Table 1). Moreover, water has important effects on chemical shifts of close by ^{1}H and ^{13}C nuclei. Last, but not least, sp^3 hybridized CH$\cdots\pi$ contacts, although of minor importance in the energetics, are sensitive detectors of the hydration/dehydration of CIP.

■ ASSOCIATED CONTENT

Ⓢ Supporting Information

Crystal structures of **II** and **III** (CIF) and details of NMR data and chemical shift calculations. This material is available free of charge via the Internet at http://pubs.acs.org.

■ AUTHOR INFORMATION

Corresponding Author

lmafra@ua.pt

■ ACKNOWLEDGMENTS

The authors thank Fundação para a Ciência e a Tecnologia (FCT) for continued funding of the project PTDC/QUIQUI/100998/2008 and the Portuguese National NMR Network (RNRMN). The postdoc grants to S.S. and R.S. are also acknowledged. We thank CICECO (Univ. Aveiro), POCTI, FEDER, and FSE. L.M. greatly acknowledges the Max-Planck Society for funding. We also thank Lyndon Emsley for providing access to the PSMN computer cluster and D. Sebastiani and M. Hansen for fruitful discussions.

■ REFERENCES

(1) Desiraju, G.; Steiner, T. *The Weak Hydrogen Bond in Structural Chemistry and Biology*; Oxford University Press: New York, 2001.
(2) Brown, S.; Spiess, H. *Chem. Rev.* **2001**, *101*, 4125.
(3) Yates, J.; Pham, T.; Pickard, C.; Mauri, F.; Amado, A.; Gil, A.; Brown, S. *J. Am. Chem. Soc.* **2005**, *127*, 10216.
(4) Uldry, A.-C.; Griffin, J. M.; Yates, J. R.; Perez-Torralba, M.; Maria, M. D. S.; Webber, A. L.; Beaumont, M. L. L.; Samoson, A.; Claramunt, R. M.; Pickard, C. J.; Brown, S. P. *J. Am. Chem. Soc.* **2008**, *130*, 945.
(5) Bradley, J. P.; Velaga, S. P.; Antzutkin, O. N.; Brown, S. P. *Cryst. Growth Des.* **2011**, *11*, 3463.
(6) Tsuzuki, S. *Struct. Bonding* **2005**, *115*, 149.
(7) Toth, G.; Bowers, S. G.; Truong, A. P.; Probst, G. *Curr. Pharm. Des.* **2007**, *13*, 3476.
(8) Reddy, J. S.; Ganesh, S. V.; Nagalapalli, R.; Dandela, R.; Solomon, K. A.; Kumar, K. A.; Goud, N. R.; Nangia, A. *J. Pharm. Sci.* **2011**, *100*, 3160.
(9) Turel, I.; Bukovec, P.; Quiros, M. *Int. J. Pharm.* **1997**, *152*, 59.
(10) Fabbiani, F. P. A.; Dittrich, B.; Florence, A. J.; Gelbrich, T.; Hursthouse, M. B.; Kuhs, W. F.; Shankland, N.; Sowa, H. *CrystEngComm* **2009**, *11*, 1396.
(11) Febles, M.; Perez-Hernandez, N.; Perez, C.; Rodriguez, M. L.; Foces-Foces, C.; Roux, M. V.; Morales, E. Q.; Buntkowsky, G.; Limbach, H.-H.; Martin, J. D. *J. Am. Chem. Soc.* **2006**, *128*, 10008.
(12) Vogt, F. G.; Brum, J.; Katrincic, L. M.; Flach, A.; Socha, J. M.; Goodman, R. M.; Haltiwanger, R. C. *Cryst. Growth Des.* **2006**, *6*, 2333.
(13) Sakellariou, D.; Lesage, A.; Hodgkinson, P.; Emsley, L. *Chem. Phys. Lett.* **2000**, *319*, 253.
(14) Zhao, X.; Hoffbauer, W.; auf der Günne, J. S.; Levitt, M. H. *Solid State Nucl. Magn. Reson.* **2004**, *26*, 57.
(15) Sebastiani, D. *ChemPhysChem* **2006**, *7*, 164.